Available online at www.sciencedirect.com
SCIENCE DIRECT®
Journal of Power Sources 140 (2005) 226–234
JOURNAL OF POWER SOURCES
www.elsevier.com/locate/jpowsour

# Viable image analyzing method to characterize the microstructure and the properties of the Ni/YSZ cermet anode of SOFC

K.-R. Lee, S.H. Choi, J. Kim, H.-W. Lee, J.-H. Lee*

*Nano-Materials Research Center, Korea Institute of Science and Technology, Seoul 136-791, Republic of Korea*

Received 21 May 2004; accepted 22 June 2004
Available online 8 December 2004

**Abstract**

The quantitative analysis of the microstructure and related physicochemical properties of the anode substrate are essential for the identification of the optimum fabrication conditions for the best performance of the SOFC unit cell. However it is not easy to characterize the correlation of the microstructure and the property of the Ni/YSZ cermet anode due to its very complicated structural features. Moreover, it is not a simple matter to differentiate all of the phases in the Ni/YSZ anode via simple microscopic observations. In this study, we developed an image analyzing method to differentiate each constituent phase of the Ni/YSZ cermet, enabling us to investigate the microstructural evolution of the Ni/YSZ anode and the characterization of the correlation between the microstructure and the properties of the Ni/YSZ anode.


*Keywords:* SOFC; Ni/YSZ anode; Image analysis; Microstructure analysis

## 1. Introduction

The commonly used Ni/YSZ cermet is known to have many desirable properties for use in SOFC anodes, such as high electronic and ionic conductivity, high electrochemical activity, and good microstructural stability. The electrical property and/or electrochemical properties of Ni/YSZ cermet anodes are normally controlled not only by the electrical conductivity of the metal-ceramic composite itself but also by the appropriate gas diffusion path, in order to reduce the ohmic and diffusional polarization losses of the cell performance, respectively [1–5].

Both the electrical conductivity and the gas permeability of SOFC anodes are strongly related to microstructural parameters, for example, the particle size, composition and spatial distributions of the constituent phases [4,5]. However, it is not easy to characterize the correlation of the microstructure and the properties of the Ni/YSZ cermet anode due to very complicated structural features with three different phases: metallic Ni, YSZ ceramic and pores.

In our previous study [6], we showed it was feasible to conduct a quantitative image analysis of the anode microstructure to characterize the correlation of the microstructure and the properties of the anode. Nonetheless, it was not a simple matter to differentiate all of the phases in an anode substrate via simple microscopic observations [7–10] because the backscattered coefficients of Ni and YSZ phases were too much alike. Thus, we had to use somewhat indirect methods to separate the information about the phases: (1) information about the Ni phase was separated from the optical micrograph, based on the large difference of the brightness between Ni and the other phases; (2) pores were separated from the other solid phases via SEM micrograph; and (3) the YSZ phase was separated by etching out the Ni phase with hydrochloric acid.

Such an indirect and multiple-step method is very complicated and inconvenient to carry out, even if somewhat meaningful microstructural information can be obtained. In addition, this method often results in inaccurate microstructural

* Corresponding author. Tel.: +82 2958 5532; fax: +82 2958 5529.
*E-mail address:* jongho@kist.re.kr (J.-H. Lee).

0378-7753/$ – see front matter © 2004 Elsevier B.V. All rights reserved.
doi:10.1016/j.jpowsour.2004.06.031

information, because the data from each characterization step is from different samples and different sample-preparation methods for the stereological observations. Thus, many efforts have been made to develop a simple and straightforward method to differentiate all three phases simultaneously.

Recently, Simwonis et al. [7] reported a very efficient method to identify all of the phases in the Ni/YSZ anode, by controlling the brightness of certain anode components. In their study, they modified the polished surface of the Ni/YSZ cermet via the selective sputtering of a $Fe_2O_3$ interference film to the Ni phase, which led to a decrease of Ni contrast and the successful discrimination of each phase.

However, the experiments of Ref. [7] were very difficult to perform and to reproduce, because the thickness of the coated interference layer is too difficult to control, to acquire a suitably high level of contrast between the different phases. Thickness control of the coated interference layer is very crucial: if the layer is too thin, the brightness of the Ni particles will be too high; consequently, the contrast between YSZ and the pores will be disturbed. On the contrary, if the layer is too thick, then the contrast between Ni and YSZ will be reduced, making clear separation of the two phases unachievable, due to similar brightness of each phase.

In this study, we propose a viable and simple method to analyze quantitatively each of the constituent microstructural features, including size, distribution and the contiguousness of the Ni, YSZ, and pore phases in the Ni–YSZ anode substrate. A proper way of analyzing the complicated structure–property–processing correlation of the SOFC anode will also be discussed.

## 2. Experiments

For the fabrication of anode substrate, we used NiO (Sumitomo, USA), coarse YSZ (Unitec, UK) and fine YSZ (Tosho, Japan) with a mixing ratio of 56:22:22 wt.% as the starting materials. The average particle sizes of the fine YSZ, the coarse YSZ, and the NiO were 0.25, 1.8 and 0.8 μm, respectively. The pre-mixed powders were ball-milled in the proper solvents for 24 h and then granulated to aid powder compaction at the forming stage. In this study, we used a liquid condensation process for the granulation and used a thermoset polymer as both a deformable fugitive phase and binder, which provided additional porosity after the heat treatment. The granules of the NiO/YSZ mixture were compacted and uni-axially pressed into a plate with 8 cm × 8 cm area, of ∼1 mm in thickness, under a pressure ranging from 4 to 16 MPa, in order to get different microstructural features of the anode substrate.

With an optical microscope (Zeiss Axiovert, Germany), we investigated the microstructures of the Ni/YSZ cermet, which had been reduced at 900 °C, for 3 h, in a reducing atmosphere. We prepared the Ni/YSZ cermet sample, following a general ceramographic method. At this point, we used some special techniques to preserve the original microstructure of the Ni/YSZ cermet, because the porous (in our case, above 20% up to 50% of porosity) structure of the Ni/YSZ cermet can be easily damaged during grinding and polishing. According to our previous microstructural investigation of the Ni/YSZ cermet, a relatively soft Ni metal phase was easily mashed during the grinding and polishing process resulting in the misinterpretations of the microstructure, especially with regard to the pore structure of Ni/YSZ cermet.

To avoid such damage of the Ni/YSZ cross-section, we used a polymer infiltration method similar to that of Simwonis et al. [7]. In their study [7], they filled a porous Ni/YSZ cermet with an epoxy resin to create a rigid skeleton that kept the pore structure intact during the polishing. However, an epoxy resin is difficult to remove after polishing. Therefore, we investigated various polymeric phases and eventually developed a proper polymer blend. The developed polymer blend is easier to infiltrate into a porous body, and leaves no unfilled space, which makes it very useful for the investigation of a nano-porous body. The polymer blend also provides more rigidity than an epoxy polymer when polishing, and it is easy to remove after polishing.

After hardening of the infiltrated polymer phase, grinding and polishing were carried out with SiC paper and diamond pastes down to 1 μm particles. An optical microscope (Zeiss Axiovert, Germany), equipped with a digital camera (JVC KY-F70, Japan), was used to capture digital images of the Ni/YSZ cermet. With this system, we translated the optical images into digitized pixels with 255 different gray values (0 for black and 255 for white pixels).

Image analysis with Image-Pro (Media Cybernetics, USA), based on quantitative microscopic theory, was performed to separate each of the constituent phases and to quantify various microstructural parameters of each phase, such as size, distribution, and contiguity of each phases. The electrical conductivities of the Ni/YSZ cermet were measured by means of dc four-point probe technique with a current source (Keithley 224, USA) and a DMM (Keithley 2000, USA). The porosity and gas permeability of the samples were measured with a mercury porosimeter (Micrometrics, USA) and perm porometer (PMI, USA), respectively. All of these measurements were performed to verify the quantitative image analysis of the Ni–YSZ anodes.

## 3. Results and discussion

In our previous study [6], we pointed out that the quantitative analysis of the microstructure and related physicochemical properties of the anode substrate are most essential for the identification of the optimum fabrication conditions for the best performance of the unit cell. However, as we mentioned in the previous section, the main obstacle of this analysis exists from the first stage of the microscopic observation.

Fig. 1 shows typical SEM micrographs of the Ni/YSZ cermet. As shown in Fig. 1a, all the solid phases showed the same brightness, and it was not possible to differentiate the Ni

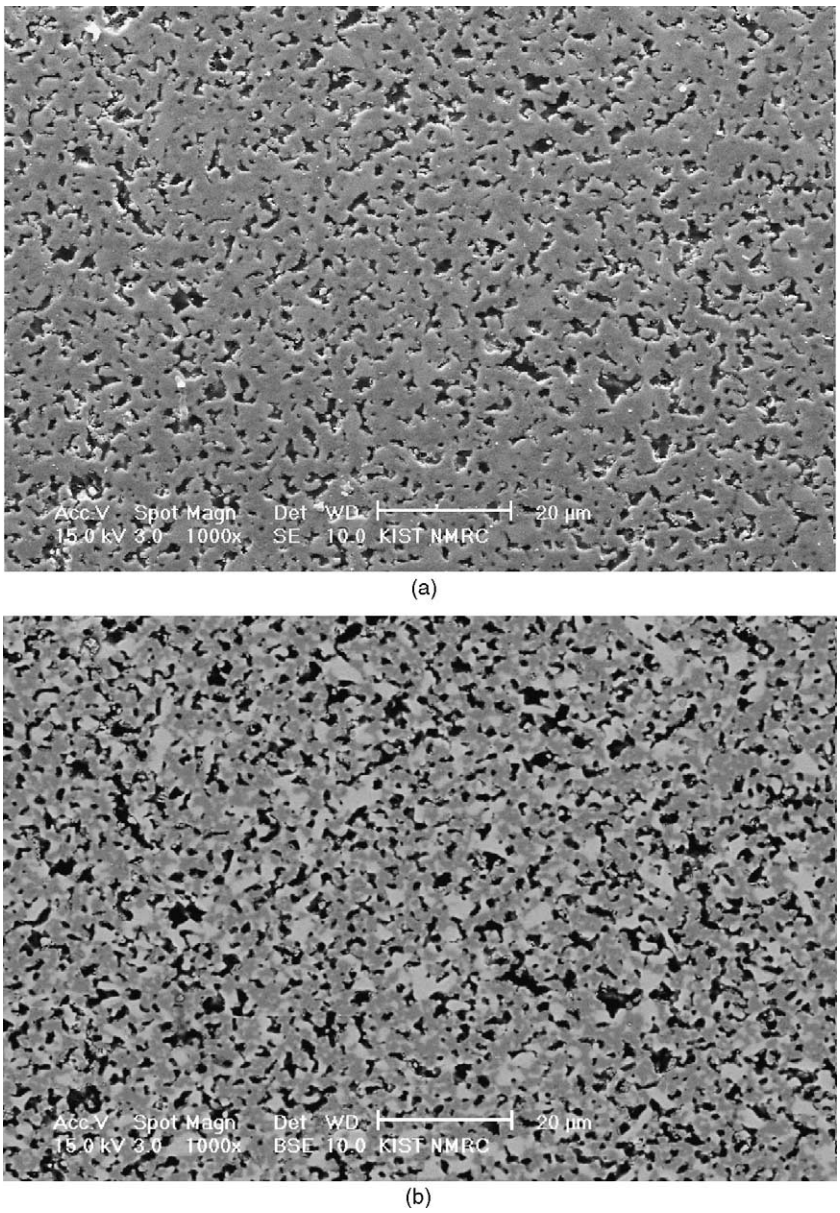


Fig. 1. Cross-sectional views of Ni/YSZ cermet: (a) SEM image; (b) BSE image.

phase from the YSZ phase. In addition, the BSE image cannot visibly separate the Ni phase from the YSZ phase (Fig. 1b). On the other hand, the general optical image of the Ni/YSZ cermet in Fig. 2 showed an extremely high brightness of the Ni phase, contrasted with the YSZ phase and pore phase, causing an insufficient difference in darkness to distinguish the pore phase from the YSZ phase.

Therefore, we developed a very simple and viable method to differentiate each phase of the Ni/YSZ cermet from a single micrograph, without any surface treatment of the Ni/YSZ cermet. A typical micrograph of the Ni/YSZ cermet anode and its gray-scale value histogram are given in Fig. 3. As shown in Fig. 3, the range of gray-scale value is too narrow to be distinguished and only the brightness of the Ni phase is clearly distinguished from the other phases. Therefore, the first step of the image development is the contrast enhancement of the original image. We used Photoshop software (Adobe, USA) to control the contrast of the image.

In Fig. 4, a contrast-enhanced digital image of Ni/YSZ and its gray-scale value histogram are given. As shown in Fig. 4, the contrast has been enhanced, compared with original image in Fig. 3, and the resulting range of the gray-scale value is extended to a full range. However, there are still some unclear boundaries remaining between the different brightnesses in Fig. 4. Thus, the second step of the image development is noise filtering via the graphic tools of Photoshop. In this operation, we reduced the frame of observation by trimming some edge parts of the actual image out, for better resolution of analysis, because the unclear contrast was observed mainly on these edge parts. For this step, we fixed the image

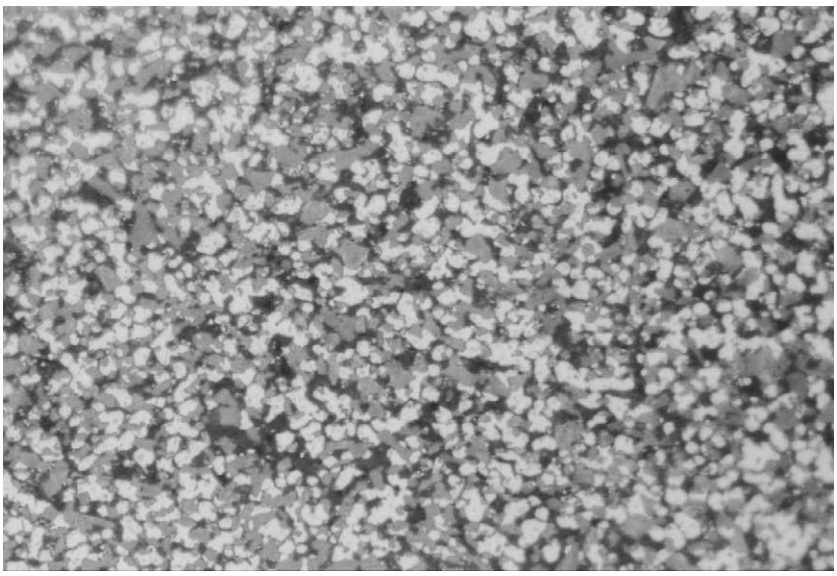

Fig. 2. Typical optical micrograph of Ni/YSZ cermet.

size of investigation at 40 μm × 33 μm for whole through the analysis.

The resulting image of Ni/YSZ and its gray-scale value histogram are given in Fig. 5. As shown in Fig. 5, the contrast between the different phases is enhanced, resulting in relatively dark images of pores, relatively bright images of Ni, and intermediate brightness of the YSZ images, which is suitable for better resolution of the phase separation. As the

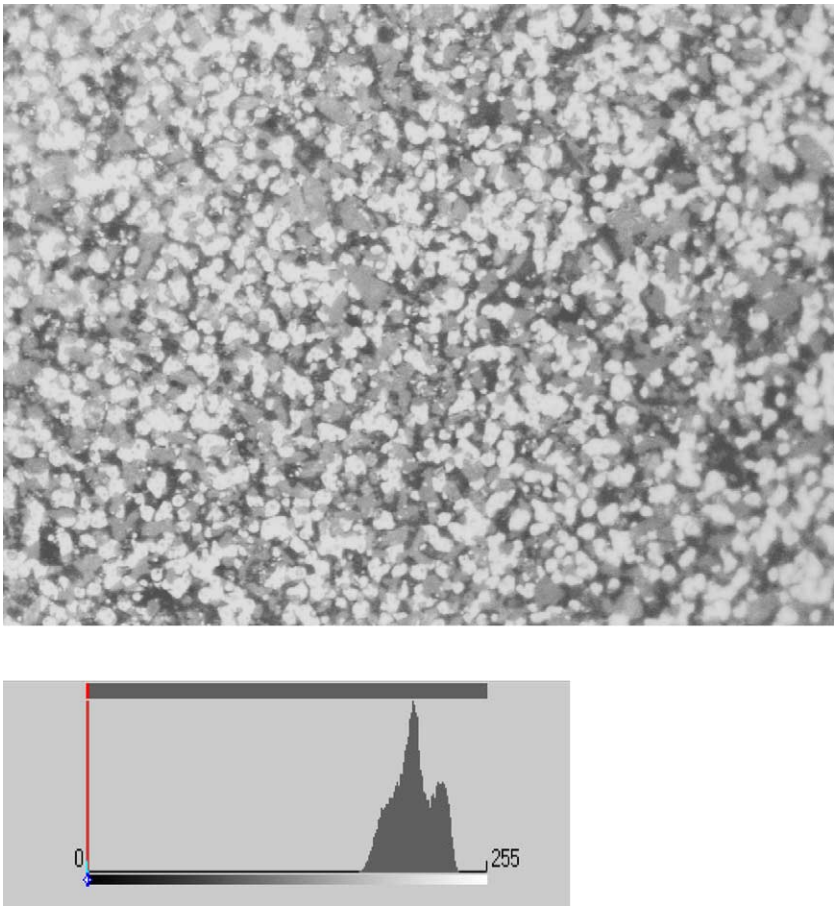


Fig. 3. Optical micrograph and a gray-scale value of a Ni/YSZ cermet (gray value 0 = black, 255 = white).

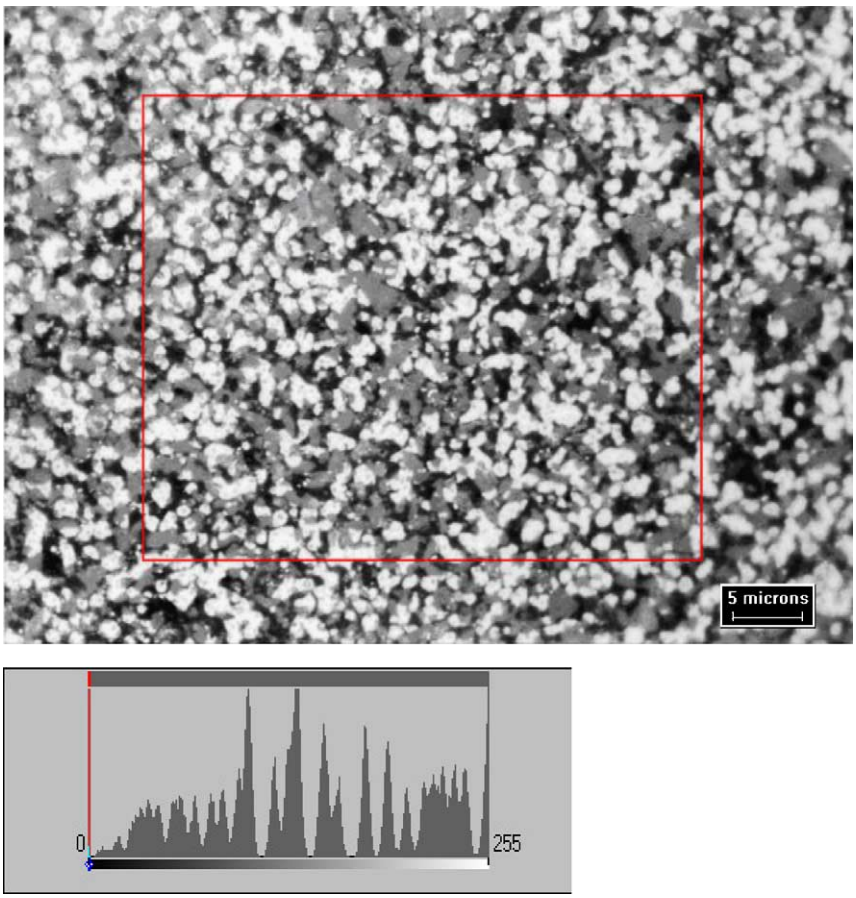


Fig. 4. Contrast-enhanced image and a gray-scale value of a Ni/YSZ cermet (gray value 0 = black, 255 = white).

next step of the analysis for the exact differentiation of each phase, we adopted a specific threshold value of brightness, with a tolerance of 30% for each phase; the resulting image and its gray-scale value histogram are shown in Fig. 6. For better visualization of the separated images we applied coloration to each of the phases. The resulting colorized ternary image is shown in Fig. 7, where the exact discrimination of the Ni, YSZ, and the pores is made possible by using different colors.

We separated independent binary images containing only one selected phase from ternary image in Fig. 7 for further detailed microstructural analysis. As shown in Fig. 8, the separated images of each Ni, YSZ and pore phase are very clearly differentiated and are suitable for the quantitative analysis of each corresponding phase. The entire process of the image analysis for the original optical micrograph is shown in Fig. 9 in the form of flow chart.

With these de-convoluted binary images, we applied the line-interception method as the main analyzing tool to characterize the microstructural parameters of the composite, such as the size, the distribution, and the contiguity of the selected phases, in order to investigate a more specific microstructure–property correlation. As the main sequence of line interception, we introduced multi-parallel lines for each *x*- and *y*-direction of the two-dimensional images to measure

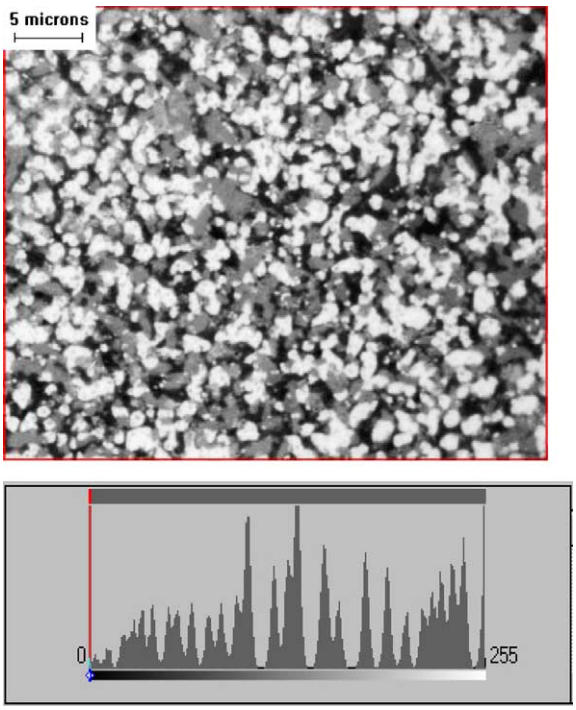


Fig. 5. Digital image after noise filtering and the gray-scale value of a Ni/YSZ cermet (gray value 0 = black, 255 = white).

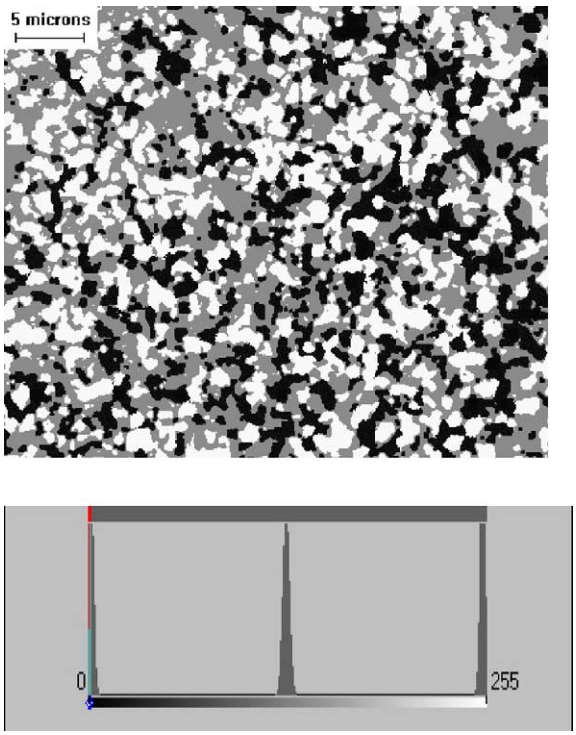


Fig. 6. Optimized digital image with three different gray-scale values.

the interception length of the selected phase on the line, a procedure that is also useful to investigate the anisotropy of each phase. To assure the reliability of the analysis, we introduced at least 100 independent parallel lines for each direction in more than 10 digital images. In order to process the large quantity of analysis data, we used automatic line-intercept analyzing programs with Image-Pro software. From this synthetic analysis, we could guarantee that the maximum error of the analysis would be less than 5%. The details of the line-interception method were already introduced elsewhere [6].

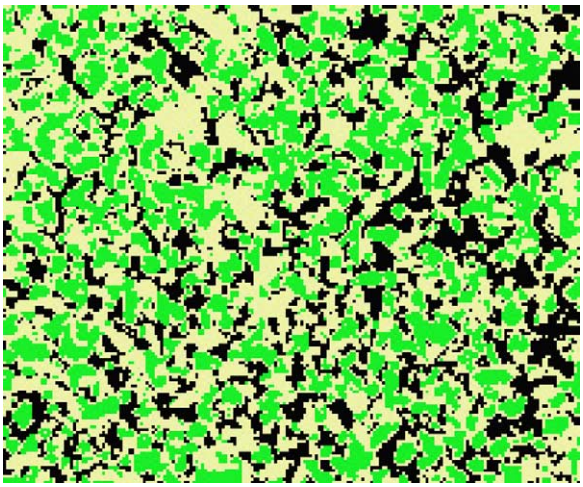

Fig. 7. Coloration of digital image with three different colors.

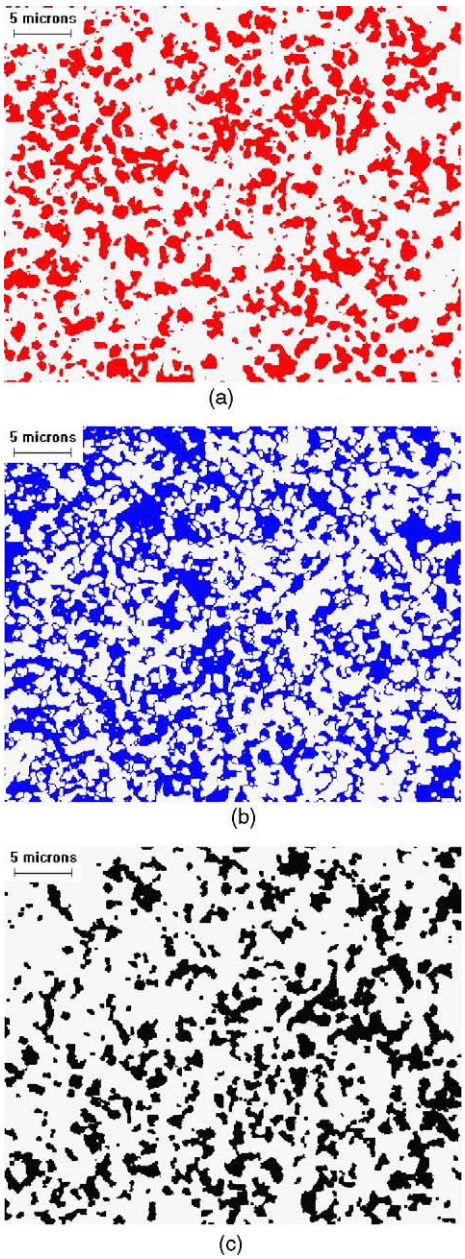


Fig. 8. Separation of three different phases of Ni/YSZ cermet and resulting binary images: (a) Ni; (b) YSZ; (c) Pores.

To check the validity of our line-intercept analysis, the results of the area fractions of three phases are plotted in Fig. 10 and compared with the reference data. As shown in Fig. 10, the theoretical values of the Ni and YSZ area fraction, which were calculated from the initial composition of the Ni/YSZ cermet, corresponded well to the estimated fraction from the image analysis. Furthermore, the estimated value of porosity from the image analysis also corresponded well to actual measurements via the Archimedes method and mercury porosimetry. These results provide assurance that our image analyzing method is very consistent and reliable.

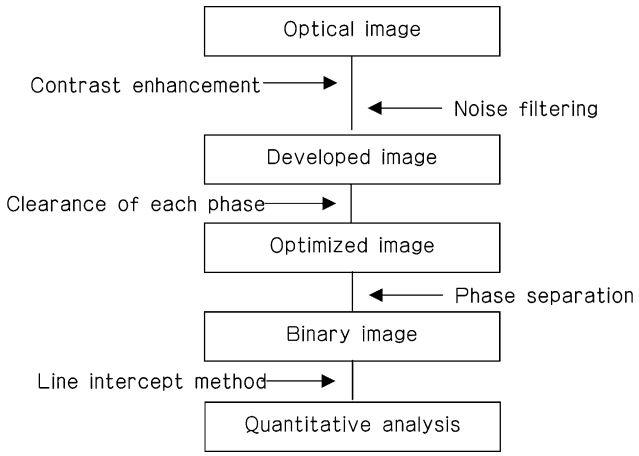


Fig. 9. Schematic flow chart of the image analysis process.

Nonetheless, in principle, all these results, such as the size and area fraction of the Ni, the YSZ, and the pore phases from the image analysis provided only two-dimensional information. Thus, for the calculation of three-dimensional contiguity of selected phase, from which we could derive a more direct correlation with the physical properties of the Ni/YSZ cermet, we introduced a quantitative stereological theory [11–14] and transformed the two-dimensional information to three-dimensional information, in a quantitative manner.

According to Simwonis et al. [7] the microstructural information from a two-dimensional micrograph can be transformed to three-dimensional structural information based on quantitative stereological theory [11–14]. In their study, they proposed following equations to calculate the three-dimensional contiguity ($C_i$) of a selected phase from the fraction of the contact areas ($S_v^i$) of the phase $i$ (=Ni, YSZ, pores) relative to the total inner surface, which had been originally adopted for the two phase mixtures [15–18].

$$C_i = \frac{S_v^i}{\sum_i S_v^i} \tag{1}$$

In this equation, the volume to surface area ratio ($V_i/S_v^i$) of phase $i$ can be defined as

$$\frac{V_i}{S_v^i} = \frac{l_i}{4} \tag{2}$$

where $l_i$ is the intercept length of the phase $i$ derived from the line-interception analysis of the two-dimensional images.

From Eqs. (1) and (2), the three-dimensional contiguities of each selected phase are expressed as the following:

$$C_{\mathrm{Ni}} = \frac{V_{\mathrm{Ni}} l_{\mathrm{YSZ}} l_{\mathrm{pore}}}{V_{\mathrm{Ni}} l_{\mathrm{YSZ}} l_{\mathrm{pore}} + V_{\mathrm{YSZ}} l_{\mathrm{Ni}} l_{\mathrm{pore}} + V_{\mathrm{pore}} l_{\mathrm{Ni}} l_{\mathrm{YSZ}}} \tag{3.1}$$

$$C_{\mathrm{YSZ}} = \frac{V_{\mathrm{YSZ}} l_{\mathrm{Ni}} l_{\mathrm{pore}}}{V_{\mathrm{Ni}} l_{\mathrm{YSZ}} l_{\mathrm{pore}} + V_{\mathrm{YSZ}} l_{\mathrm{Ni}} l_{\mathrm{pore}} + V_{\mathrm{pore}} l_{\mathrm{Ni}} l_{\mathrm{YSZ}}} \tag{3.2}$$

$$C_{\mathrm{pore}} = \frac{V_{\mathrm{pore}} l_{\mathrm{YSZ}} l_{\mathrm{Ni}}}{V_{\mathrm{Ni}} l_{\mathrm{YSZ}} l_{\mathrm{pore}} + V_{\mathrm{YSZ}} l_{\mathrm{Ni}} l_{\mathrm{pore}} + V_{\mathrm{pore}} l_{\mathrm{Ni}} l_{\mathrm{YSZ}}} \tag{3.3}$$

As shown in Eqs. (3.1)–(3.3), the three-dimensional information of contiguity can be calculated from the two-dimensional structural parameter of the intercept length and the volume fraction obtained from the image analysis of the two-dimensional micrograph. The calculated values of three-dimensional contiguity for all three components of Ni/YSZ cermet are plotted in Fig. 11 as a function of one of the typical processing variables, $P$ (compaction pressure). As shown in Fig. 11, the variation of the contiguity with respect to the

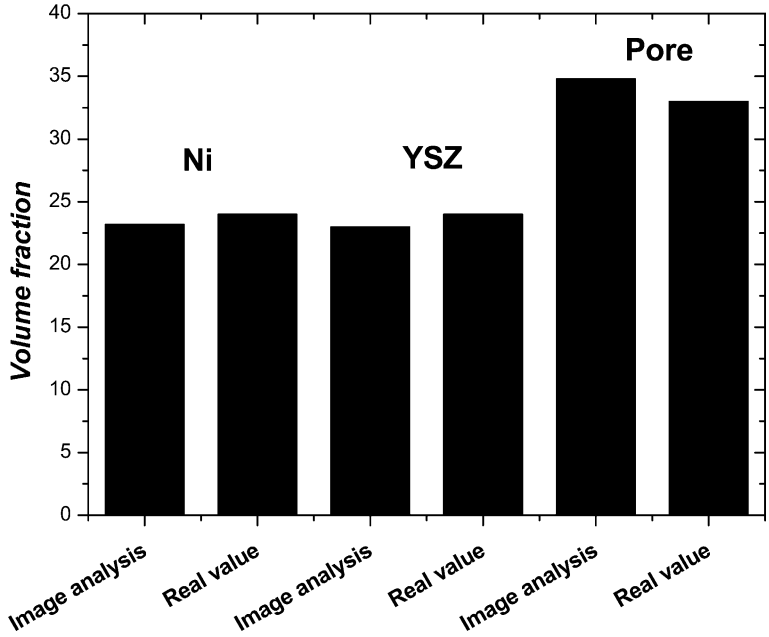


Fig. 10. Comparison of the volume fractions of constituent phase from the image analysis and the real estimated values.

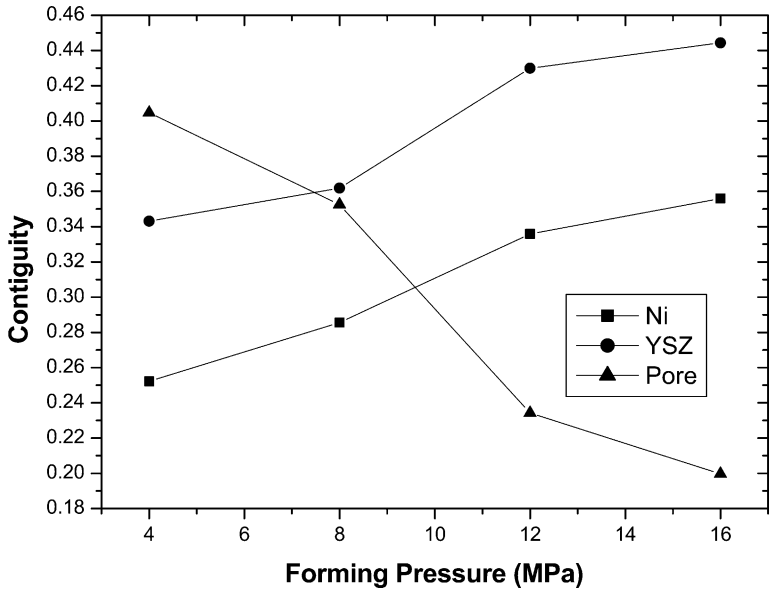


Fig. 11. The three-dimensional contiguity of the Ni, YSZ, and pores with respect to the forming pressure.

compaction pressure agrees with our initial expectation that the contiguity of solid phases, Ni and YSZ, increases, and the pore contiguity decreases as the compaction pressure increases.

As we emphasized in our previous study [6], the contiguity of each constituent component of the Ni/YSZ cermet is very important for the prediction of the electrodic functions of an SOFC anode. To verify the importance of this contiguity, we investigated the correlation of contiguity with the corresponding physical properties of Ni/YSZ cermet.

We plotted the calculated values of the Ni and the pore contiguities with their corresponding electrical conductivities and gas permeabilities (Figs. 12 and 13). As we expected, the three-dimensional contiguity of a selected phase shows a very strong correlation with its corresponding physical properties. The electrical conductivity of the Ni/YSZ cermet, which is the main factor of ohmic polarization, was mostly controlled by the appropriate connection of the conducting phase, Ni. The gas permeability, which is a main factor of diffusional polarization loss, was controlled by the appropriate connection of the gas diffusion path, pores.

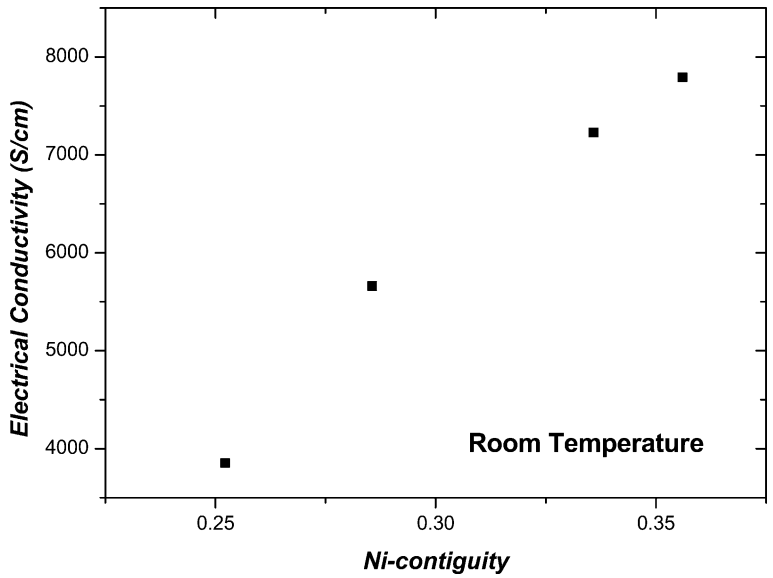


Fig. 12. Correlation of the Ni contiguity and corresponding electrical conductivity.

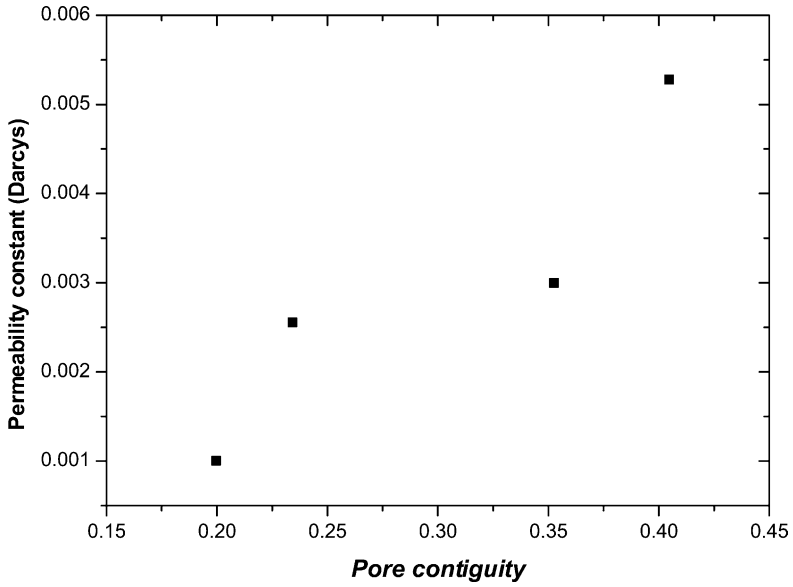


Fig. 13. Correlation of the pore contiguity and corresponding gas permeability.

## 4. Conclusions

A proposed image analyzing method was found to be a very viable means to investigate the microstructural evolution of a multi-component composite electrode, specifically the Ni/YSZ anode of SOFC. The quantified microstructural data from image analysis, which included the size, the distribution, and the contiguity of each constituent phase, were very helpful to understand the very complicated microstructural features of the three different phases of Ni/YSZ. A combined microstructural analysis with an image analysis and a corresponding physical property measurement were very valuable for the investigation of the correlation between the microstructure and the property. We expect that this characterization method will consequently enable us to optimize the microstructure and property of the Ni/YSZ anode for the best performance of SOFC.

## Acknowledgements

This work was partially supported by the Korea Institute of Science and Technology Evaluation and Planning (KISTEP) through the National Research Laboratory (NRL).

## References

[1] A. McEvoy, in: S.C. Singhal, K. Kendall (Eds.), High Temperature Solid Oxide Fuel Cells, Elsevier, UK, 2003, p. 149.
[2] X. Deng, A. Petric, in: S.C. Singhal, M. Dokiya (Eds.), Proceedings of the Eighth International Symposium Solid Oxide Fuel Cells (SOFC-VIII), The Electro chemical Society, Pennington, NJ, 2003, p. 653.
[3] C. Kalyvas, N. Brandon, R. Collins, in: J. Huijsmans (Ed.), Proceedings of the Fifth European Solid Oxide Fuel Cell Forum, European Fuel Cell Forum, 2002, p. 539.
[4] D.-S. Lee, J.-H. Lee, J. Kim, H.-W. Lee, H.S. Song, Solid State Ionics 166 (2004) 13.
[5] J.-H. Lee, J.-W. Heo, D.-S. Lee, J. Kim, G.-H. Kim, H.-W. Lee, J.-H. Moon, Solid State Ionics 158 (2003) 225.
[6] J.-H. Lee, H. Moon, H.-W. Lee, J. Kim, J.-D. Kim, K.-H. Yoon, Solid State Ionics 148 (2002) 15.
[7] D. Simwonis, F. Tietz, D. Stoever, Solid State Ionics 132 (2000) 241.
[8] F. Meschke, F.J. Dias, F. Tietz, J. Mater. Sci. 36 (2001) 5719.
[9] D. Simwonis, A. Naoumidis, F.J. Dias, J. Linke, A. Moropoulou, J. Mater. Res. 12 (1997) 1508.
[10] M. Mogenson, S. Primdahl, J.T. Rheinländer, S. Gormsen, S. Linderoth, M. Brown, in: M. Dokiya, O. Yamamoto, H. Tagawa, S.C. Singhal (Eds.), Proceedings of the Fourth International Symposium on Solid Oxide Fuel Cells (SOFC-IV), The Electro chemical Society, Pennington, NJ, 1995, p. 657.
[11] J. Gurland, Trans. Metall. Soc. AIME 212 (1958) 452.
[12] J. Gurland, Trans. Metall. Soc. AIME 236 (1966) 642.
[13] Z. Fan, Philos. Mag. A 73 (1996) 1663.
[14] Z. Fan, A.P. Miodownik, P. Tsakiropoulos, Mater. Sci. Technol. 9 (1993) 1094.
[15] K.B. Alexander, P.F. Becher, S.B. Waters, A. Bleier, J. Am. Ceram. Soc. 77 (4) (1994) 939.
[16] E.E. Underwood, Stereologia 3 (1964) 5.
[17] C.S. Smith, L. Guttman, Trans. Metall. Soc. AIME 197 (1953) 81.
[18] J.W. Cahn, J.E. Hilliard, Trans. Metall. Soc. AIME 215 (1959) 759.